J. Membrane Biol. 161, 115–129 (1998)

The Journal of
Membrane
Biology

The Estimation of Rapid Rate Constants from Current-Amplitude Frequency Distributions of Single-Channel Recordings

P.J. White[1], **M.S. Ridout**[2]

[1]Department of Cell Physiology, Horticulture Research International, Wellesbourne, Warwick CV35 9EF, UK
[2]Department of Biometrics, Horticulture Research International, East Malling, West Malling, Kent ME19 6BJ, UK

Received: 4 October 1996/Revised: 2 September 1997

Abstract. A method is described for estimating rapid rate constants from the distributions of current amplitude observed in single-channel electrical recordings. It has the advantages over previous, similar approaches that it can accommodate both multistate kinetic models and adjustable filtering of the data using an 8-pole Bessel filter. The method is conceptually straightforward: the observed distributions of current amplitude are compared with theoretical distributions derived by combining several simplifying assumptions about the underlying stochastic process with a model of the filter and electrical noise. Parameters are estimated by approximate maximum likelihood. The method was used successfully to estimate rate constants for both a simple two-state kinetic model (the transitions between open and closed states during the rapid gating of an outward-rectifying K^+-selective channel in the plasma membrane of *Acetabularia*) and a complex multistate kinetic model (the blockade of the maxi cation channel in the plasma membrane of rye roots by verapamil). For the two-state model, parameters were estimated well, provided that they were not too fast or too slow in relation to the sampling rate. In the three-state model the precision of estimates depended in a complex way on the values of all rate parameters in the model.

Key words: *Acetabularia* — Blockade — Channel kinetics — Gating — K^+ channel — Maxi cation channel — Rye (*Secale cereale* L.) — Verapamil

Introduction

The temporal analysis of currents obtained from an individual ion channel provides a means both to investigate intrinsic changes in the conformation of the channel protein itself and to identify the mechanisms of interactions between the channel protein and its effectors. The aim of such analyses is to determine the kinetic schemes underlying, for example, the process of channel gating or the mechanism of ionic blockade of an ion channel. In addition to providing an empirical description, such information suggests a mechanistic interpretation by which to compare information on protein sequence and structure.

Several methods are available for estimating the lifetimes of distinct kinetic states of an ion channel, and the rate constants for transitions between each state, from single-channel current records. Such records can be thought of as resulting from the superimposition of experimental noise on an underlying process that consists of transitions between different current levels. One widely used method of analysis begins by attempting to reconstruct the noise-free record. This can be done by filtering the data with a high-order Bessel filter and using threshold detection (Colquhoun, 1994), by using a high-order Hinkley detector (Schultze & Draber, 1993; Draber & Schultze, 1994) or by using a Bayesian approach (Fredkin & Rice, 1992*b*). Rate parameters can then be estimated from the distributions of dwell times at the various current levels, though the analysis is complicated by the fact that short dwell times will be missed by the restoration process (e.g., Ball & Davies, 1995). This approach works well if the mean lifetimes of the kinetic states are lengthy, but as mean lifetimes decrease the method eventually becomes unreliable, because there are too many missed events. Typically, this occurs when mean lifetimes are 10–100 μsec, depending on the extent of experimental noise and filtering, and on the sampling frequency of the recording equipment.

An alternative, and more direct approach, is to model the observed current record directly, without attempting to restore the underlying process (Fredkin & Rice, 1992*a*; Albertsen & Hansen, 1994). This appears

Correspondence to: P.J. White

to be a promising approach, but it is computationally intensive and therefore not presently well-suited to the analysis of large numbers of current records.

Lifetimes of channel conformations between 1 msec and 1 μsec (this value depending upon the filter time constant) can be estimated from current-amplitude frequency distributions. These become distorted from a Gaussian to an asymmetric distribution, which approximates a beta distribution, within this temporal range (Yellen, 1984; Pietrobon, Prod'hom & Hess, 1989; Klieber & Gradmann, 1993). Lifetimes of kinetic states have been estimated from current-amplitude frequency distributions both empirically for two-state kinetic models, by comparing simulated and experimental data (Yellen, 1984; Pietrobon et al., 1989; Klieber & Gradmann, 1993), and numerically, for multistate kinetic models when data have been filtered by a single-pole filter (Rießner & Hansen, 1995). If the lifetime of a channel conformation is shorter than a microsecond, analysis based on beta distributions can no longer be applied. Lifetimes of brief kinetic states are obtained either by comparing the noise of different channel conformations (Heinemann & Sigworth, 1988), or from the analysis of the higher-order cumulants of the current-amplitude distribution (Heinemann & Sigworth, 1991).

In this paper a method of estimating the lifetimes of channel conformational states which lie between about 30 msec and 1 μsec is described. This method is based on the analysis of distributions of current amplitude and may be viewed as an extention of analyses based on beta distributions. It has the advantages over previous approaches that it can accommodate both multistate kinetic models and the filtering of data using an 8-pole Bessel filter. In the approach described here the theoretical distribution of current amplitude is derived directly by combining several simplifying assumptions about the underlying stochastic process with a model of the filter and electrical noise. The approach has been used successfully to estimate rate constants for both a simple two-state kinetic model, the transitions between open and closed states during the rapid gating of an outward-rectifying K^+-selective channel in the plasma membrane of *Acetabularia acetabulum* (White, Smahel & Thiel, 1993), and a complex multistate kinetic model, the blockade of the maxi cation channel in the plasma membrane of rye (*Secale cereale* L.) roots by verapamil (White, 1996).

Materials and Methods

Ion Channel Recordings

Plasma membrane vesicles from *Acetabularia acetabulum* (White et al., 1993) or from rye (*Secale cereale* L.) roots (White & Tester, 1992) were incorporated into planar lipid bilayers (PLB; 0.2 mm in diameter) composed of 30 mM synthetic 1-palmitoyl-2-oleoyl phosphatidylethanolamine dispersed in n-decane. The side of the PLB to which vesicles were added was defined as *cis*. Experimental protocols used to characterize the voltage-dependence of the 149 pS (chord conductance at E_{rev} in 100 mM KCl) K^+ channel from *Acetabularia* plasma membrane are given in White, Smahel & Thiel (1993) and those used to determine the effects of verapamil on the maxi cation channel in the plasma membrane of rye roots are given in White (1996). Voltages are expressed *trans* with respect to *cis*. It was assumed that the cytoplasmic side of the plasma membrane faces the vesicle lumen and that vesicles fuse with PLB such that the inside becomes exposed to the *trans* chamber (White & Tester, 1992, 1994). Thus, the sign of the membrane potential is in accordance with the physiological convention (Bertl et al., 1992). Movement of cations from the *cis* (extracellular) to the *trans* (cytoplasmic) compartment is indicated by a negative current and appears as a downward deflection in current traces. This convention has the opposite polarity to that used in previous studies characterizing the maxi cation channel in the plasma membrane of rye roots in PLB (White & Tester, 1992; White, 1993, 1996).

Current through individual ion channels was monitored under voltage-clamp conditions using a low noise operational amplifier with frequency compensation (Miller, 1982), connected to the bilayer chambers by calomel electrodes and 3 M KCl/1% agar salt bridges. Data were stored either on videotape after digitizing by a Sony audio-to-digital converter (PCM-701ES, 22 kHz per channel; Sony, Japan), for experiments with the *Acetabularia* K^+ channel, or on Digital Audio Tape (Sony DTC-1000ES; 44.1 kHz sampling with 16-bit linear digital to analog conversion) for experiments with the maxi cation channel from rye roots. For analysis, recordings of channel activity were replayed and filtered using an 8-pole tunable low pass Bessel filter (902LPF, Frequency Devices, Haverhill, MA) set at 4 kHz (corner frequency on dial). The operational amplifier itself also filtered the data, with a cutoff frequency that we estimated as about 2.25 kHz. The combined effect of these filters was approximated as a single Bessel filter (Colquhoun & Sigworth, 1983) with a cutoff frequency

$$\sqrt{\frac{1}{\frac{1}{4^2}+\frac{1}{2.25^2}}} = 1.96 \text{ kHz}$$

which, given the uncertainty about the cutoff frequency of the operational amplifier, has been taken as 2 kHz.

The impulse response function of the Bessel filter was approximated by a Gaussian probability density function (Colquhoun & Sigworth, 1983). Small weights were set to zero and the remaining weights were rescaled to sum to one. The number of non-zero weights in the impulse response function was 9 for data stored on videotape and 15 for data stored on Digital Audio Tape. Increasing the number of non-zero weights resulted in a smoother distribution of current amplitudes and the use of fewer non-zero weights may result in a rippling in the simulated distribution, such as that observed in Fig. 2*D*. The filtered data were sampled by computer after digitization to 12 bit accuracy using a CED 1401plus (Cambridge Electronic Design, Cambridge, UK) at 11 kHz (i.e., effectively ever second or every fourth value from the filtered data was sampled).

Modelling the Distribution of Current

The general approach of Yellen (1984) in modelling the distribution of current was followed. A basic mathematical result, due to FitzHugh (1983), is that if a 2-state (open-blocked) Markov process, with fixed and known currents in the two states, is filtered with a first-order filter, the resulting distribution of current is a beta distribution. The param-

eters of the beta distribution are related to the transition rates between the two states and to the time constant of the filter.

This result is of limited practical value for three reasons: it assumes a linear filter, it ignores any noise in the current, and it applies only to a two-state process. Yellen (1984) addressed the first of these problems empirically. He used simulation to investigate the effect of using instead an 8-pole Bessel filter and found that, over a wide range of opening and blocking rates, the distribution of current remained approximately beta-distributed, with the beta distribution parameters modified according to the −3dB attenuation frequency of the filter. He also superimposed Gaussian noise on the beta distribution. He then fitted the resulting distribution by eye. This approach has been followed by several subsequent authors (e.g., Pietrobon et al., 1989; Klieber & Gradmann, 1993).

More recently, Rießner & Hansen (1995) have investigated the extension of FitzHugh's basic result when the underlying process has more than two states. However, the differential equations analogous to those which lead to the beta distribution for the two-state model cannot be solved analytically in the more general case and must instead be solved numerically.

The approach used in the present paper was instead to make some simplifying assumptions about the underlying stochastic process and to combine this with a model of the filter to derive the distribution of current directly. This approach is conceptually straightforward and computationally feasible.

Stochastic Model of the Channel

The temporal behavior of the channel was modelled as a continuous time Markov process with S states, of which S_O are open and $S - S_O$ are closed (Colquhoun & Hawkes, 1981). The process is characterized by the matrix $Q = (q_{ij})$ where, for $i \neq j$, q_{ij} is the transition rate from state i to state j, and where

$$q_{ii} = -\sum_{i \neq j} q_{ij}$$

Two well-known results from the theory of Markov processes were utilized (Cox & Miller, 1965, Section 4.5). First, if $p_{ij}(\Delta t)$ denotes the probability that the channel is in state j at time $t + \Delta t$, given that it was in state i at time t (because the process is assumed to be a Markov process, this *transition probability* depends only on Δt and not on t itself), the matrix $P(\Delta t) = (p_{ij}(\Delta t))$ of transition probabilities is related to the matrix of transition rates, Q, by the equation

$$P(\Delta t) = \exp(\Delta t Q)$$

This matrix exponential can be evaluated in various ways (Moler & Van Loan, 1978). The approach of Horn & Lange (1983) was followed, using a truncated Taylor series expansion and rescaling the matrix Q, where necessary, to improve accuracy.

The second result concerns the equilibrium distribution of the channel. It was assumed that any state of the channel can eventually be reached from any other state of the channel, possibly via intermediate states. This condition is sufficient to ensure that the channel has an equilibrium probability distribution. Let e_i denote the probability that, in equilibrium, the channel is in state i, and let E denote the column vector with ith element e_i. The equilibrium probabilities can be evaluated by solving the linear equations

$$Q^{\mathrm{T}} E = 0$$

subject to the constraint that the probabilities must sum to one.

Equilibrium Probability of a Particular Sequence of States

Suppose that the channel is observed at time t and also at m preceding times, the interval between successive observation times being equal to Δt. Let the states of the channel at the successive observation times be $\{U(t - m\Delta t), U(t - (m - 1)\Delta t), \ldots, U(t)\}$. There are S^{m+1} possible sequences of states. If the channel is in equilibrium, the probability of a particular sequence is

$$e_{U(t-m\Delta t)} \prod_{j=-m}^{-1} p_{U(t+j\Delta t),U(t+(j+1)\Delta t)}(\Delta t) \qquad (1)$$

Let $\{V(t - m\Delta t), V(t - (m - 1)\Delta t), \ldots, V(t)\}$ denote the open/closed sequence arising from the sequence $\{U(t - m\Delta t), U(t - (m - 1)\Delta t), \ldots, U(t)\}$ where $V(s) = 1$ if $U(s)$ is an open state and $V(s) = 0$ if $U(s)$ is a closed state.

There are 2^{m+1} possible open/closed sequences and the probability of any particular sequence could be obtained directly by summing probabilities given by expression (1) over all underlying sequences of states which result in the given open/closed sequence. However, a much more efficient algorithm has been used for calculating probabilities of open/closed sequences, the so-called *forward algorithm*, that was developed in the literature on *hidden Markov models*. Rabiner (1989) provides a clear description of this algorithm. Several other authors (e.g., Chung et al., 1990; Fredkin & Rice, 1992*a*,*b*) have applied hidden Markov model techniques to ion channel problems.

Modelling the Observed Current

It was assumed that, before filtering, the current at time t, $X(t)$, was of the form

$$X(t) = \mu_{V(t)} + \epsilon(t)$$

where $\epsilon(t)$ is a stationary Gaussian process with zero mean. Thus, the expected current is μ_0 when the channel is closed and μ_1 when it is open. There was assumed to be no baseline drift.

The observed current at time t, $Y(t)$, results from filtering the current $X(t)$. This was modelled by the equation below. The lag l ($\geqslant 0$) was introduced to avoid complications with zero weights in the impulse response function. However, because the process is stationary, the distribution of $Y(t+l)$ is the same as that of $Y(t)$.

$$Y(t+l) = \sum_{k=0}^{m} a_k X(t - k\Delta t)$$

The sequence $\{a_0, \ldots, a_{m-1}, a_m\}$ is a discrete approximation to the impulse response function of the filter with $a_k > 0$ and

$$\sum_{k=0}^{m} a_k = 1$$

For a *particular* open/closed sequence $\{V(t - m\Delta t), V(t - (m - 1)\Delta t), \ldots, V(t)\}$ the distribution of observed current, $Y(t)$, is itself Gaussian, with mean

$$\sum_{k=0}^{m} a_k \mu V(t - k\Delta t) \qquad (2)$$

and with variance σ^2. The *unconditional* distribution of current is

therefore a mixture of 2^{m+1} Gaussian distributions, with varying mean but constant variance, the proportion of each component of the mixture being the probability of the corresponding open/closed sequence.

A particular implication of this model, which is borne out by the experimental data, is that the distribution of current whilst the channel is open or closed should be Gaussian, with a standard deviation that is not dependent on the state of the channel.

To speed up some of the computations, the following approximation was employed. Instead of working with the mixture of 2^{m+1} Gaussian distributions, a mixture of R Gaussian distributions was generated with the same variance and with means equally spaced on the interval $[\mu_0,\mu_1]$. The probability of a particular component in the new mixture with mean μ^* is the sum of the probabilities assigned to all components in the original mixture whose mean is closer to μ^* than to the mean of any other component in the new mixture. The values $m = 8$ and $m = 14$ were taken for data stored on videotape and DAT tape, respectively. Thus, the original mixtures had either 512 or 32768 components. A 65-fold saving in computational effort was obtained when $m = 14$ by taking R as 500. The loss of accuracy resulting from this approximation is very slight because each exact mean is replaced by an approximate mean, μ^*, which differs from it by at most 0.1% of the difference $\mu_1 - \mu_0$.

Statistical Analysis

Since the distribution of current comprises a mixture of Gaussian distributions which can be evaluated once the rate parameters, q_{ij}, and the parameters μ_0, μ_1 and σ are known, the observed distribution of current can be used, in principle at least, to estimate these parameters. Because channel records often consist of 10^5–10^6 observations it is computationally efficient to work with grouped frequency data rather than individual current measurements. Therefore, the current values were grouped into B bins, with bin limits $b_0 = -\infty, b_1, b_2, \ldots, b_{N-1}, b_N = \infty$, and n_k denotes the number of observed currents in the interval (b_{k-1}, b_k). Provided that B is reasonably large, there should be little loss of efficiency in using grouped data rather than ungrouped data. In practice B was approximately 50, with all of the internal bins having equal width ($b_k = b_{k-1} + \Delta b$, $k = 2, \ldots, B-1$), but it is not essential to use bins of equal width.

Parameters were estimated by an approximate maximum likelihood method. To calculate the likelihood the probabilities

$$\theta_k = Pr(b_{k-1} \leqslant Y(t) < b_k) \quad k = 1, 2, \ldots, B$$

need to be evaluated and, because the distribution of current is a mixture of Gaussian distributions, these probabilities are simply mixtures of Gaussian probabilities. The underlying Gaussian probabilities depend only on the parameters μ_0, μ_1 and σ, whereas the mixture coefficients depend solely on the rate parameters (q_{ij}) which determine the equilibrium probablities and transition probabilities required to evaluate expression (1).

Estimation of the rate parameters was the primary objective. Both μ_0 and σ were estimated directly from current recordings, during a lengthy closure or blockade of the channel. The difference $\mu_1 - \mu_0$ was estimated similarly, from current recordings obtained in the absence of any blocker at each voltage, and this was used to estimate μ_1 when a blocker was present. Using these estimates of μ_0, μ_1 and σ, the probabilities θ_k for each of the R components of the mixture of Gaussian distributions were precomputed and stored. A table that showed which component of the mixture resulted from each of the 2^{m+1} open/closed sequences was formed. This enabled the calculation of probabilities θ_k fairly quickly, given a set of rate parameters.

A multinomial distribution was assumed for the observed frequencies, n_k, so that estimates were obtained by maximizing the log-likelihood function

$$\sum_{k=1}^{B} n_k \ln(\theta_k)$$

Strictly speaking the observed frequencies do *not* have a multinomial distribution, because successive observations are not independent and it is in this sense that the method is referred to as *approximate* maximum likelihood. However, the range over which observations are correlated will generally be very short in relation to the length of the channel record, and the effects of non-independence are therefore expected to be slight.

The probablities θ_k are very complicated functions of the underlying parameters, and to maximize the log likelihood it is therefore preferable to use an optimization algorithm that does not require derivatives of the objective function. The Nelder-Mead simplex algorithm (Nelder & Mead, 1965) has been used here. For a 3-state model, with four rate parameters to be estimated and with $m = 14$, our computer program, written in Fortran 77 and running on a 100 MHz Pentium PC, takes about 0.5 sec per iteration. Fitting a distribution typically takes less than 5 min of computing time.

Limitations of the Method

It is important to consider the range of rate parameters for which the method is able to give useful estimates. This will depend on the sampling frequency, the filter cutoff frequency and the amount of underlying noise. To investigate this quantitatively a simple two-state model was considered, with rate paramters $\lambda_1 (= q_{12})$ and $\lambda_2 (= q_{21})$ between the two states. For statistical analysis it is useful to consider the natural logarithms of these rates, $\gamma_1 = \ln(\lambda_1)$ and $\gamma_2 = \ln(\lambda_2)$, rather than the rates themselves. One advantage of this is that parameters can be estimated using an unconstrained, rather than a constrained, optimization routine. But also, because the rates are constrained to be positive, estimates are likely to be more symmetrically distributed on the logarithmic scale, particularly for small rates. This in turn means that inferences based on standard errors of the logarithms of the rates are likely to be more reliable than inferences based on the standard errors of the rates themselves.

To derive standard errors of γ_1 and γ_2 the Fisher information matrix was calculated, based on the multinomial log-likelihood function

$$L(\gamma_1,\gamma_2) = \sum_{k=1}^{B} n_k \ln(\theta_k)$$

By a standard result in multinomial likelihood theory, the information matrix has (i,j)th element

$$-E\left[\frac{\partial^2 L(\gamma_1,\gamma_2)}{\partial\gamma_i\partial\lambda_j}\right] = N\sum_{k=1}^{B}\frac{1}{\theta_k}\frac{\partial\theta_k}{\partial\gamma_i}\frac{\partial\theta_k}{\partial\gamma_j}$$

where $E[.]$ denotes expectation and $N = \Sigma n_k$.

The inverse of this 2×2 matrix, whose elements are denoted by v_{ij}, is the variance covariance matrix of the maximum likelihood estimates of γ_1 and γ_2. To study how various factors affect the precision of the method the standard errors of $\ln(\lambda_1/\lambda_2) = \gamma_1 - \gamma_2$ and $\ln(\lambda_1\lambda_2) = \gamma_1 + \gamma_2$ were calculated. These are given by the following formulae

$$se[\ln(\lambda_1/\lambda_2)] = \sqrt{v_{11} + v_{22} - 2v_{12}}$$

$se[\ln(\lambda_1\lambda_2)] = \sqrt{v_{11} + v_{22} + 2v_{12}}$

These formulae depend on the data only through the total number of observations, *N*. Because only the relative values of the standard errors were of interest, and not their absolute values, $N = 1$ was taken. For any other value of *N*, standard errors should be divided by $\sqrt{N}$.

A chi-squared goodness of fit statistic can be calculated from the observed and expected number of observations in each bin, possibly pooling together bins in which the expected number of observations is very small. Because *N* is usually large (of the order of 10^5 or 10^6) this will give an extremely sensitive goodness-of-fit statistic and 'significant' departures from the assumed model will often be detected. This lack of fit may well be of little practical importance and may arise, for example, through slight mismodelling of the filter or because of minor departures from stationarity in the underlying process. However, standard errors derived in the manner outlined will be too small. A simple correction, which has been used in the examples discussed later in this paper, is to multiply the standard errors by a heterogeneity factor, calculated by dividing the chi-squared statistic by its degrees of freedom, and taking the square root (McCullagh & Nelder, 1989, p. 175). But again, this type of correction does not affect the relative values of standard errors for different true parameter values, which is presently of interest.

The standard errors of $\ln(\lambda_1/\lambda_2)$ and $\ln(\lambda_1\lambda_2)$ are plotted against the rate parameter λ_1 for four values of the other rate pararmeter λ_2 (0.1, 1, 10, 100 $msec^{-1}$; note that $msec^{-1}$ = kHz) in Fig. 1. Standard errors were calculated for different sampling rates (22 kHz or 44.1 kHz), different cutoff frequencies for filtering (1 kHz or 2 kHz) and different values of σ as a proportion of the unitary current (0.025 or 0.25).

The standard error of $\ln(\lambda_1/\lambda_2)$ is minimized when $\lambda_1 = \lambda_2$. Taking a sampling frequency of 22 kHz, a filtering cutoff frequency of 2 kHz and a standard deviation of 0.025 times the unitary current as standard (Fig. 1*C*), doubling the sampling frequency (Fig. 1*A*) or halving the filter cutoff frequency (Fig. 1*G*) both tend to reduce the standard error, but the effects are very slight. In these graphs the standard error remains relatively small for λ_2 in the range $(\lambda_1/100, 100\lambda_1)$. Increasing the underlying standard deviation tenfold (Fig. 1*E*) reduces this range to about $(\lambda_1/10, 10\lambda_1)$.

Taking the same standard conditions (Fig. 1*D*), the standard error, of $\ln(\lambda_1\lambda_2)$ is reduced by halving the filter cutoff frequency when λ_1 and λ_2 are small, but increased when they are large (Fig. 1*H*), though again the effects are quite small. However, doubling the sampling frequency reduces the standard error when either λ_1 or λ_2 is small, and the effect is more substantial (Fig. 1*B*). Increasing the underlying standard deviation tenfold again has a substantial effect (Fig. 1*F*), with the standard error increasing rapidly when either λ_1 or λ_2 moves outside the interval (1,10).

From Fig. 1 as a whole it is apparent that, at least for λ_1 and λ_2 in the range (0.01, 100), the standard error of $\ln(\lambda_1/\lambda_2)$ is dependent primarily on the value of $\ln(\lambda_1/\lambda_2)$, and not on the individual values of λ_1 and λ_2 themselves. The value of $\ln(\lambda_1/\lambda_2)$ can be estimated quite well provided λ_1 and λ_2 are not too different. In contrast, $\ln(\lambda_1\lambda_2)$ is best estimated when neither λ_1 nor λ_2 is too small or too large. It is thus estimation of the product of the rates, rather than their ratio, which sets the limitations of the method.

A small number of simulations, designed to investigate the performance of the method under ideal conditions, were also performed. Data were simulated for both the two-state and the three-state kinetic models described later in this paper. The simulation procedure had three steps. First, the state of the channel at each time point was simulated, using transition probabilities determined from the rate parameters of the model. The current at each time point was then set to μ_0 or μ_1 depending on whether the channel was open or blocked, to give a noise-free signal. The second step added random noise to the signal. The noise in our experimental setup appears to have a quadratic spectral density function and Gaussian noise with the appropriate spectrum was simulated using a program supplied by Dr. R. Levis (Rush Medical College, Chicago, IL). The third step was to filter the noisy current trace, using a Gaussian approximation to the Bessel filter. All the simulations used $\mu_0 = 0$ pA and $\mu_1 = 15$ pA, and the variability of the noise was set so that the standard deviation after filtering was 1.0 pA. In each simulation run 100,000 points were simulated initially. These were taken to represent data at 22 kHz for the two-state kinetic model and 44 kHz for the three-state kinetic model. The cutoff frequency of the Bessel filter was 2 kHz, in both instances. Sampling data by the computer, at 11 kHz, was simulated by taking every second or fourth value from the filtered series. Finally, a grouped frequency distribution was formed from the sampled currents, using 50 bins of width 0.5 pA. There were 50 simulation runs for each combination of rate parameters.

For the two-state model, conclusions based on simulations were fully consistent with those drawn from the statistical analyses described above (*data not shown*). The errors associated with rate constants in the simulated three-state model exhibited complex relationships with the true rate constants (*see* Table 1). The rate constants for the three-state model were chosen to cover the range estimated for the experimental data, and the rate constants k_{-1} and k_{-2} were unchanged also for this reason (Fig. 7). In general, as k_1 increased the ability to estimate k_2 and k_{-2} declined, but the ability to estimate k_1 and k_{-1} improved. By contrast, as k_2 increased the ability to estimate k_1 and k_{-1} declined, but the ability to estimate k_2 and k_{-2} improved. When k_2 and k_{-2} were estimated poorly, their ratio was also estimated poorly, but the ratio of the fast rates (k_1/k_{-1}) was well estimated under most simulation conditions.

Results

Estimates of Rapid Rate Constants from Experimental Data

In this section, the analysis of distributions of current amplitude has been used to estimate rate constants for both a simple two-state kinetic model (Example 1) and a complex multistate kinetic model (Example 2). In the first example, the rate constants for transitions between open and closed states during the rapid gating of an outward-rectifying K^+-selective channel in the plasma membrane of *Acetabularia* have been estimated. In the second example, the blockade of the maxi cation channel in the plasma membrane of rye roots by verapamil, which is characterized by an open state linked to two distinct blocked states, has been investigated.

Example 1. A Simple Two-State Model: The Rapid Gating Kinetics of a K^+-selective Channel in the Plasma Membrane of *Acetabularia*

When plasma membrane vesicles from *Acetabularia* are incorporated into PLB an outward-rectifying K^+-selective channel with a unitary conductance of 149 pS

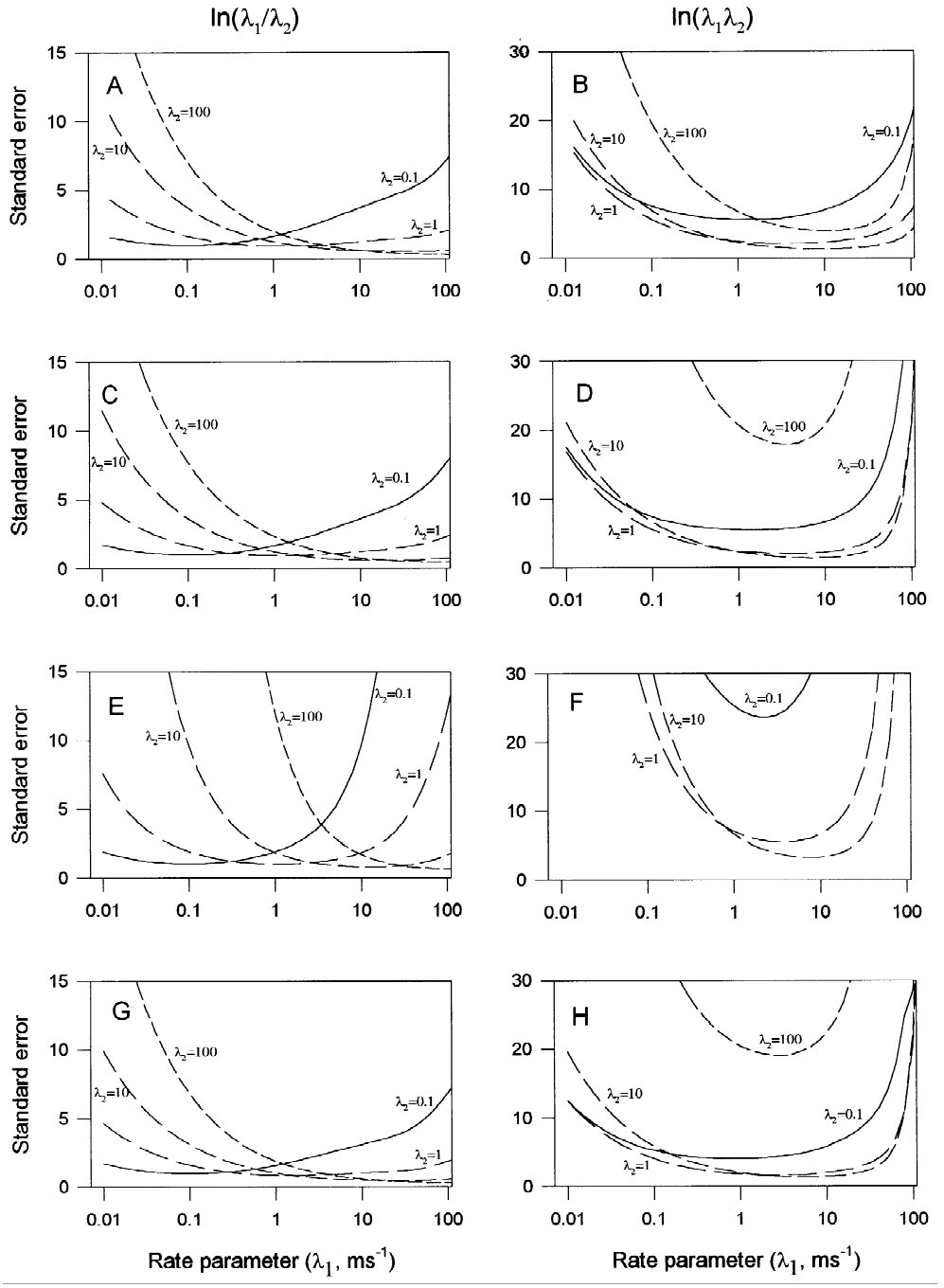

Fig. 1. Relationship between the rate parameter λ_1 in a simple two-state kinetic model and the standard errors of the natural logarithm of the ratio (left column) or product (right column) of both rate parameters for values of rate parameter λ_2 of 0.1 (——), 1 (— — —), 10 (– – –) and 100 $msec^{-1}$ (----). Values for the sampling frequency of stored data, the cutoff frequency of the Bessel filter and the signal-to-noise ratio (provided as the normalized standard deviation of the noise) were respectively: (*A* and *B*) 44.1 kHz, 2 kHz and 0.025; (*C* and *D*) 22 kHz, 2 kHz and 0.025; (*E* and *F*) 22 kHz, 2 kHz and 0.25; (*G* and H) 22 kHz, 1 kHz, 0.025.

in symmetrical 100 mM KCl is commonly observed (White et al., 1993). This channel exhibits complex kinetics. These include bursting activity (indicating the presence of at least two closed states) and, within a burst, the presence of at least two open states which differ in their mean lifetimes by over an order of magnitude, the longer one occurring rarely and noticeable only at voltages higher than 60 mV (White et al., 1993). Here the

Table 1. The relationship between the true rate constants (expressed as $msec^{-1}$) and their estimated root mean square errors

True rates ($msec^{-1}$)				RMSE (%)					
k_1	k_{-1}	k_2	k_{-2}	k_1	k_{-1}	k_2	k_{-2}	k_1/k_{-1}	k_2/k_{-2}
30	500	0.005	5	8	8	63	70	2	55
30	500	0.050	5	6	6	17	16	2	15
30	500	0.500	5	10	10	4	4	2	5
30	500	5.000	5	16	13	2	2	6	2
30	500	50.000	5	235	4039	3	3	ND	3
100	500	0.005	5	9	9	214	92	1	104
100	500	0.050	5	4	4	19	17	1	18
100	500	0.500	5	2	3	6	5	1	4
100	500	5.000	5	11	10	3	2	3	2
100	500	50.000	5	102	2065	3	4	ND	3
300	500	0.005	5	23	23	839	1637	1	47673
300	500	0.050	5	14	14	52	37	1	34
300	500	0.500	5	2	2	10	7	1	7
300	500	5.000	5	7	7	3	3	2	3
300	500	50.000	5	52	34	4	3	46	3
1000	500	0.005	5	90	101	33592	1044	2	19870
1000	500	0.050	5	25	26	7150	1312	4	11408
1000	500	0.500	5	34	33	84	50	2	29
1000	500	5.000	5	3	2	12	8	2	5
1000	500	50.000	5	23	21	7	6	13	4

RMSE are based on 50 simulations and expressed as a percentage of the true parameter value for a three-state *B1* ⇄ *O* ⇄ *B2* kinetic model. The rate constants for blockade of the open channel are indicated by k_1 and k_2, and the rates at which the channel is unblocked by k_{-1} and k_{-2}, the subscripts referring to the two independent blocked states *B1* and *B2* respectively. ND = not determined.

rate constants (k_1 and k_{-1}) for transitions between the closed (*C*) and open (*O*) states with the shortest duration are estimated:

$$C \underset{k_{-1}}{\overset{k_1}{\rightleftarrows}} O$$

The mean lifetimes of the shortest open- and closed-states of the channel are defined as τ_o and τ_c, respectively. The rate constants for transitions between these states are defined as $k_1 = 1/\tau_c$ and $k_{-1} = 1/\tau_o$. During a burst of channel activity transitions between open and closed states are extremely rapid and could not be resolved temporally even when filtered at 5 kHz (White et al., 1993). Thus, the rapid kinetics of this channel could not be analyzed using the 50%-current threshold crossing method (Colquhoun, 1994). To estimate rate constants for these rapid transitions, current amplitude frequency distributions obtained during a burst of channel activity were analyzed after excluding data attributable to long openings (Fig. 2). The standard deviation of the current noise, determined when the channel was in the closed state, was 1.10 ± 0.045 pA (mean ± SE; $n = 5$ voltages) and the relationship between unitary current and voltage is given in Fig. 2*E*.

Data were fitted with a two-state kinetic model and the fits obtained agreed well with the observed current-amplitude frequency distributions (Fig. 2*A-D*). These data also illustrate the limits of the method. The time constant for brief openings could be reliably estimated at 60 mV (when $\tau_o = 0.09$ msec, $k_{-1} = 11.51$ $msec^{-1}$ and $\tau_c = 2.57$ msec, $k_1 = 0.39$ $msec^{-1}$) but not at 50 mV (when $\tau_o = 0.10$ msec, $k_{-1} = 9.87$ $msec^{-1}$; $\tau_c = 6.17$ msec; $k_1 = 0.16$ $msec^{-1}$; estimated from Fig. 2). At 50 mV the analysis of distributions of current amplitude was compromised not only by the short k_1, but also by the worsening signal-to-noise ratio (*see* Fig. 1*E* and *F*). The value of σ/unitary current increased from 0.22 at 60 mV to 0.31 at 50 mV.

The voltage-dependence of channel P_o (Fig. 2*F*) and rate constants (k_1 and k_{-1}) obtained here (Fig. 2*G* and *H*) agree qualitatively with the results obtained when current recordings were analyzed after filtering at 100 Hz using the 50%-threshold crossing method (White et al., 1993). As expected, the rate constants obtained in the present analysis were much faster (Fig. 2*G* and *H*) and the time constants much shorter than those obtained when the traces were analyzed after filtering at 100 Hz (White et al., 1993). However, in both analyses, k_1 (and τ_c) showed a marked voltage-dependence whereas k_{-1} (and τ_o) showed only a weak voltage dependence. In the present paper, the voltage-dependence of P_o could be fitted to a Boltzmann distribution with a $V_{1/2}$ (the voltage at which P_o was half-maximal) of 108 mV and a gating charge (z)

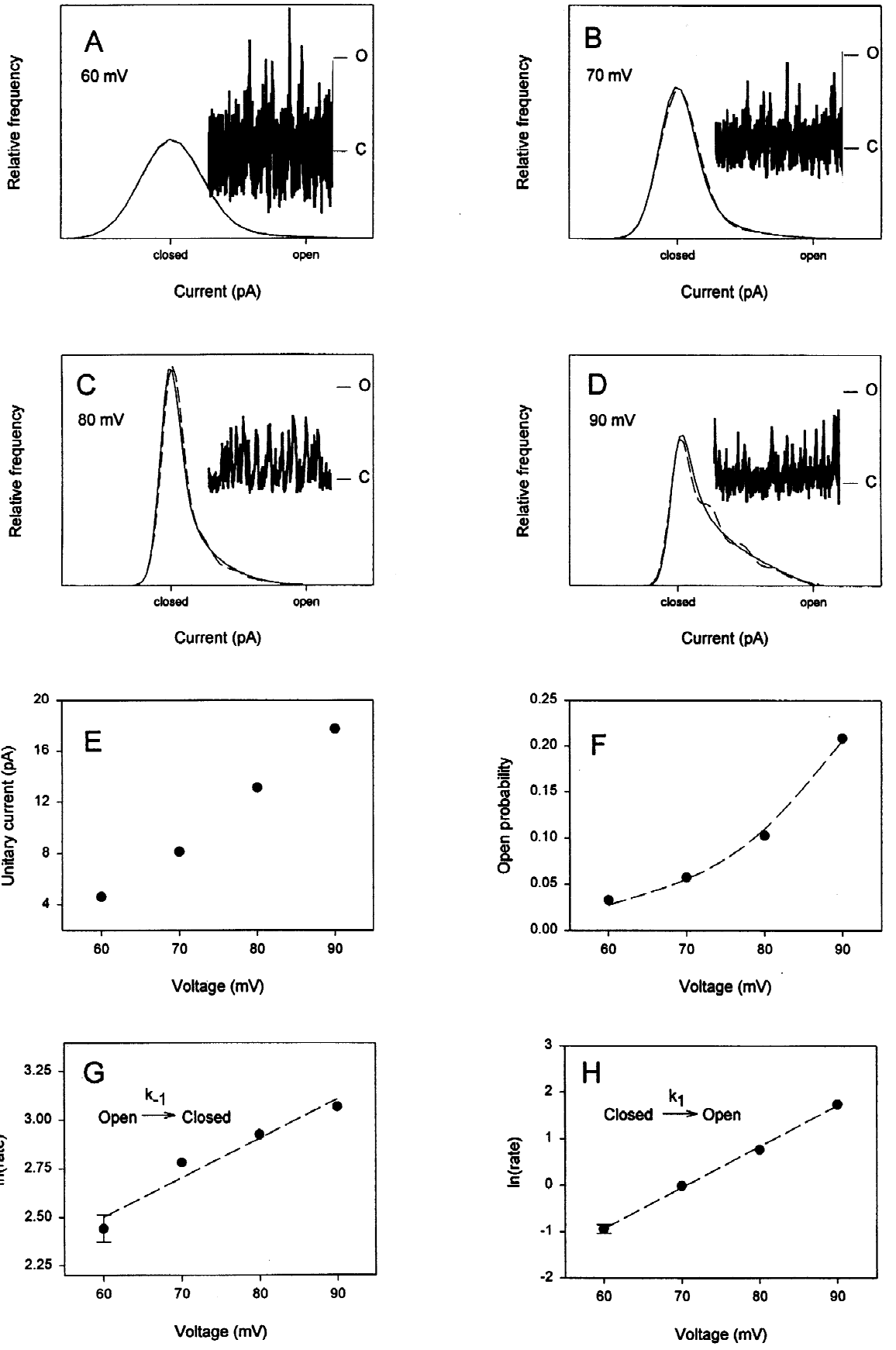
A
60 mV
O
C
Relative frequency
closed
open
Current (pA)
B
70 mV
C
80 mV
D
90 mV
E
Unitary current (pA)
20
16
12
8
4
60
70
80
90
Voltage (mV)
F
Open probability
0.25
0.20
0.15
0.10
0.05
0.00
G
k-1
Open → Closed
ln(rate)
3.25
3.00
2.75
2.50
2.25
H
k1
Closed → Open
3
2
1
0
-1
-2

Figure 2.

of 1.9. These values differ from the values obtained by White et al. (1993; $V_{1/2} = 170$ mV, $z = 1$) since more openings were detected in the present experiments.

Example 2. A Complex Multistate Model: The Blockade of the Maxi Cation Channel in the Plasma Membrane of Rye Roots by Verapamil

When plasma membrane vesicles from rye roots are incorporated into PLB a cation channel with a unitary conductance of between 425 to 451 pS in symmetrical 100 mM KCl is observed (White & Tester, 1992; White, 1993, 1996). In view of its high conductance this channel has been termed a 'maxi' cation channel (White, 1993). In addition to its maximal conductance conformation, this channel exhibits several rarely occupied subconductance states approximating 93% and 12% of the maximum conductance (White, 1993). In generating current-amplitude frequency distributions we have excluded periods when the channel was in a subconductance state.

Verapamil blocks the maxi cation channel in a voltage-dependent manner at micromolar concentrations when applied from the *trans* (cytoplasmic) side of the channel (White, 1996). Verapamil blockade of the channel becomes more pronounced as the voltage is driven to increasingly positive values. When verapamil is applied to the *cis* (extracellular) compartment, the inhibition of the maxi cation channel has a similar voltage-dependency (P.J. White, *unpublished data*). Since verapamil is lipid soluble, and believed to interact with the channel in its cationic form, these observations imply that verapamil interacts with the maxi cation channel solely from the *trans* (cytoplasmic) side.

Unipolar, voltage-dependent inhibition of cation channels by verapamil is commonplace. Both the L-type Ca^{2+} channels in the plasma membrane of animal cells (Catterall & Striessnig, 1992; Hille, 1992; Ertel & Cohen, 1994) and the outward-rectifying K^+ channel in the plasma membrane of tobacco protoplasts (Thomine et al., 1994) are inhibited more effectively by verapamil at more positive voltages; and verapamil inhibition of a Ca^{2+}-selective channel in the plasma membrane of wheat roots increases with increasingly negative voltages (Piñeros & Tester, 1995).

In the absence of verapamil, the maxi cation channel remains open at low positive voltages for lengthy periods (minutes) without closure (White, 1993). As the voltage is driven more positive there is an increase in the frequency of transitions between the open and closed states of the channel (White, 1993). However, even at extreme positive voltages the gating kinetics of the maxi cation channel are slow. Therefore, most periods during which the channel is in a closed state can be identified in current recordings and have been eliminated from the analysis of current amplitude frequency distributions. Any unnoticed closures should have negligible effect on the shape of the open state current-amplitude distribution. Thus, the current-amplitude frequency distributions represent transitions between open and blocked states of the channel only.

Verapamil induces both fast and intermediate blockade of the channel, reducing the apparent unitary current through the channel as well as introducing flickering to the current recording (White, 1996). This implies that the interaction between the channel protein and verapamil produces at least two blocked states, which will be termed *B1* and *B2*. The analysis of distributions of current amplitude has been used to determine the kinetic relationships between the open channel and these blocked states. The rate constants for blockade of the open channel by verapamil are indicated by k_1 and k_2, and the rates at which the channel is unblocked by k_{-1} and k_{-2}, the subscripts referring to *B1* and *B2* respectively. Experiments were performed with 100 mM KCl on both sides of the channel and the relationship between unitary current and voltage in an unblocked channel is shown in Fig. 3. The standard deviation of current noise, determined when the channel was in the closed state, was 1.01 ± 0.021 (mean ± SE; $n = 47$ determinations at positive voltages at verapamil concentrations between 0 and 300 μM).

The three-state model provided a significantly better fit to the current-amplitude frequency distributions than a

Fig. 2. Analysis of the kinetics of the 149 pS K^+ channel in the *Acetabularia* plasma membrane assayed in asymmetrical (*cis:trans*) 325:100 mM KCl. (*A–D*) Observed (——) and fitted (---) current frequency distributions at 60 , 70, 80, and 90 mV. Channel open- and closed-states are indicated. Rate constants for fitted distributions are shown in panels *G* and *H*, unitary currents in panel *E* and the standard deviation of the current noise averaged 1.10 pA. *Inset:* Sample of the original current recordings (200 μsec in duration) filtered using an 8-pole Bessel filter set at 4 kHz. The current associated with channel open (*O*) and closed (*C*) states is indicated. (*E* and *F*) The voltage-dependencies of unitary current, open probability (calculated from the rate constants presented in panels *G* and *H*), and rate constants for channel closing (k_{-1}) and opening (k_1). The unitary currents were re-estimated and the value at 80 mV is slightly lower than that reported previously (White et al., 1993). The relationship between open probability and voltage was fitted to a Boltzmann distribution of the form $P_o = (1 + \exp\{(zF/RT)(V_{1/2} - V)\})$ where the hypothetical gating charge (z) was 1.88 ± 0.122 and the voltage at which P_o was half maximal ($V_{1/2}$) was 108 ± 1.5 mV. Rate constants ($msec^{-1}$) were fitted to an equation of the form $\ln(k) = A + BV$, where $A = 1.29 \pm 0.256$ and $B = 0.020 \pm 0.0033$ for k_{-1} and $A = -6.22 \pm 0.198$ and $B = 0.088 \pm 0.0026$ for k_1. Standard errors of rate constants are indicated by bars, when these are larger than the plotting symbols.

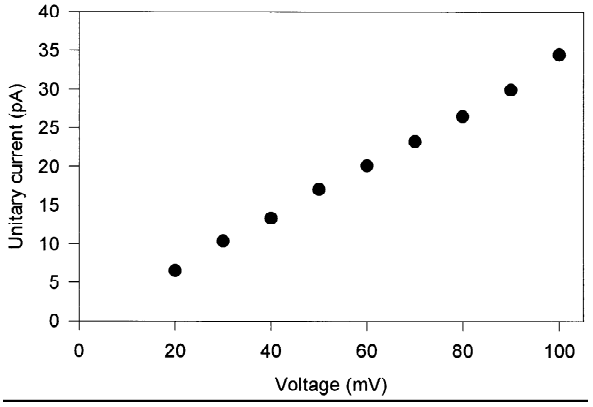

Fig. 3. The relationship between unitary current and voltage for the maxi cation channel in the plasma membrane of rye roots assayed in the presence of symmetrical 100 mM KCl.

two-state model (Fig. 4). However, since there is equivalence between contrasting three-state models, these cannot be distinguished solely on the basis of steady-state kinetic data (Kienker, 1989). Since the rates of blockade achieving both *B1* and *B2* were dependent upon the verapamil concentration in the *trans* chamber (Fig. 7), this implies that both blocked states are directly accessible from the *trans* side of the channel and are not linked in series. Therefore, the model

$$B1 \underset{k_{-1}}{\overset{k_1}{\leftrightarrows}} O \underset{k_{-2}}{\overset{k_2}{\rightleftarrows}} B2$$

is most appropriate to describe the blockade of the maxi cation channel by verapamil. Rate constants for this model were estimated, with the additional assumption that only one verapamil binding site on the protein could be occupied at any moment.

The blockade of the maxi cation channel was dependent upon both verapamil concentration and voltage (White, 1996; Figs. 5–7). When either the verapamil concentration was increased at a constant voltage (Fig. 5) or more positive voltages were imposed at a constant verapamil concentration (Fig. 6), there was a general shift towards lower normalized currents and a broadening of the current-amplitude frequency distribution. The three-state model fitted the experimental data well at higher verapamil concentrations and at more positive voltages. However, at lower verapamil concentrations and less positive voltages, the fitted current-amplitude frequency distributions were broader than those observed experimentally. It is likely that the true rate constants are slower than the estimated rate constants at lower verapamil concentrations and less positive voltages. It is possible that lengthy openings compromised these estimates: fewer changes in state occur at lower verapamil concentrations and less positive voltages, which minimizes the deviation from a Gaussian distribution. The ratio k_1/k_{-1} was well estimated under most conditions. However, the slower rate constants derived for the three-state model were more reliable at higher verapamil concentrations and more positive voltages.

The rate constants for blockade of the channel, k_1 and k_2, were dependent upon both verapamil concentration and voltage (Fig. 7). At all voltages, the relationship between k_1 and verapamil concentration followed a saturation curve, but there was no evidence of saturation for k_2. It was assumed that blockade occurred through entry of cationic verapamil to the channel pore on the basis of voltage-dependence, but, independent evidence is required to verify this. At pH 7.5 approximately 90% of the verapamil will carry a single positive charge, the remainder being uncharged (Roberts & Haigler, 1990). The voltage-dependence of each rate constant was fitted to a Boltzmann distribution (Woodhull, 1973; Eq. 2*a*). The apparent fraction of the electrical distance from the cytoplasmic side of the channel to the verapamil binding site (δ) was 0.75 for k_1 and 4.24 for k_2. A value for δ greater than unity contradicts any notion of the channel having an inflexible pore structure occupied by a single ion. Such values might be obtained if there were interactions between ions within the pore of the channel (Hille, 1992) or if access to the verapamil binding site required a voltage-dependent structural change in the channel protein (Draber & Hansen, 1994).

Neither of the rate constants for unblocking the channel, k_{-1} or k_{-2}, exhibited a comparable voltage-dependence of opposite polarity to their counterparts (Fig. 7). Thus, verapamil exited the channel protein from both its binding sites by different routes to its entry. This could be the result of a conformational change in the channel protein during verapamil binding preventing backward movement. The effect of voltage on k_{-1} was not statistically significant, suggesting that the binding site was external to the electric field or that verapamil exited *B1* in the unprotonated form. The latter mechanism has a parallel with the exit of verapamil from the pore of Ca channels in animal cells (Hille, 1992). The rate of unblocking *B2*, k_{-2}, increased significantly as the voltage was driven more positive, suggesting the exit of cationic verapamil towards the *cis* (extracellular) solution. The apparent fraction of the electrical distance from *B2* to the extracellular side of the channel (calculated using the Woodhull equation) was 0.38. Increasing verapamil concentration resulted in a significant decrease in both k_{-1} and k_{-2}, which suggests the possibility of (steric) hindrance of verapamil dissociation by verapamil in the external medium.

The equilibrium binding constant (K_d) at 0 mV was estimated as the ratio of the bimolecular blocking rate and unimolecular unblocking rate (Hille, 1992). The K_d values for *B1* and *B2* approximated 700 μM and 140 mM,

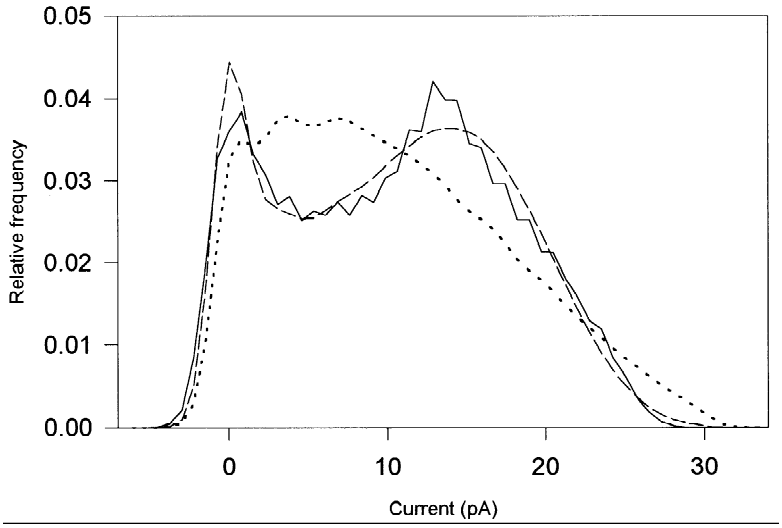

Fig. 4. Current frequency distributions obtained for the maxi cation channel from rye roots at 90 mV in the presence of 100 μM verapamil. The observed data (——) are compared with fitted distributions according to a two-state (. . . . . .) and a three-state (----) kinetic model.

respectively. Thus, although verapamil appears to be an effective blocker of the maxi cation channel at extreme positive voltages, its potency in binding studies will be minimal.

Discussion

A method of estimating rapid rate constants from the distributions of current-amplitude has been developed and used successfully to estimate rate constants for both a simple two-state kinetic model (the rapid gating kinetics of a K^+-selective channel in the plasma membrane of *Acetabularia*) and a complex multistate kinetic model (the blockade of the maxi cation channel in the plasma membrane of rye roots by verapamil). Lifetimes of distinct channel kinetic states in the range 30 msec to 1 μsec were adequately resolved in these analyses (Figs. 2 and 7). However, the absolute range of rate constants which can be reliably estimated depends upon a number of factors including the frequencies at which data is sampled for storage (on computer, DAT or videotape) and subsequently filtered, the signal-to-noise ratio and the rate constants themselves (Fig. 1). It is clear that the distribution of current varies only when the rate parameters lie within a certain range, but whether rate parameters are uniquely determined by a given current distribution has not yet been established. This is an important subject for future investigation.

The model assumes that the data are sampled and stored on video- or DAT-tape prior to filtering, and all filtering is applied to the data as they are stored. In reality, however, the implicit filtering performed by the amplifier has already been done before the data are stored. This filtering will take place at much faster effective sampling rates than modelled here. It is not possible to model filtering at such high temporal resolution at present, due to limitations in computing power. However, computational methods to extend the temporal range of the filter are being investigated. This phenomenon could result in some distortion of the predicted, relative to the actual, current frequency distributions. This will only be of serious concern for rates that are fast relative to the sampling rate. It should not affect estimates of rate parameters for the K^+ channel in the plasma membrane of *Acetabularia* and is unlikely to account for poor fits to the observed current frequency distributions for the maxi cation channel from rye roots at low voltages and in the presence of low verapamil concentrations.

The method described in this paper extends previous approaches to the analysis of current frequency distributions (Yellen, 1984; Rießner & Hansen, 1995) to accomodate both multistate kinetic models and the filtering of data with an 8-pole Bessel filter prior to analysis. The inclusion of a Bessel filter in the circuit has the advantage that the filter frequency can be changed. This allows the experimenter to adjust the shape of the current frequency distribution to maximize the temporal range over which the technique can be applied (*cf.* Klieber & Gradmann, 1993). It also allows the experimenter to analyze prefiltered data. With the patch-clamp amplifier circuit described here the analysis is unlikely to benefit much by faster sampling and/or the removal of the Bessel filter since the filtering inherent in the feedback amplifier of the patch clamp circuit (2.25 kHz) effectively limits the analysis.

The analysis of current-frequency distributions complements methods based on restoration of the underlying process or on direct modelling of current recordings. The method described here has two advantages over restoration methods. First, since the restoration methods are critically dependent upon both filtering and sampling frequencies, it has the advantage that data can

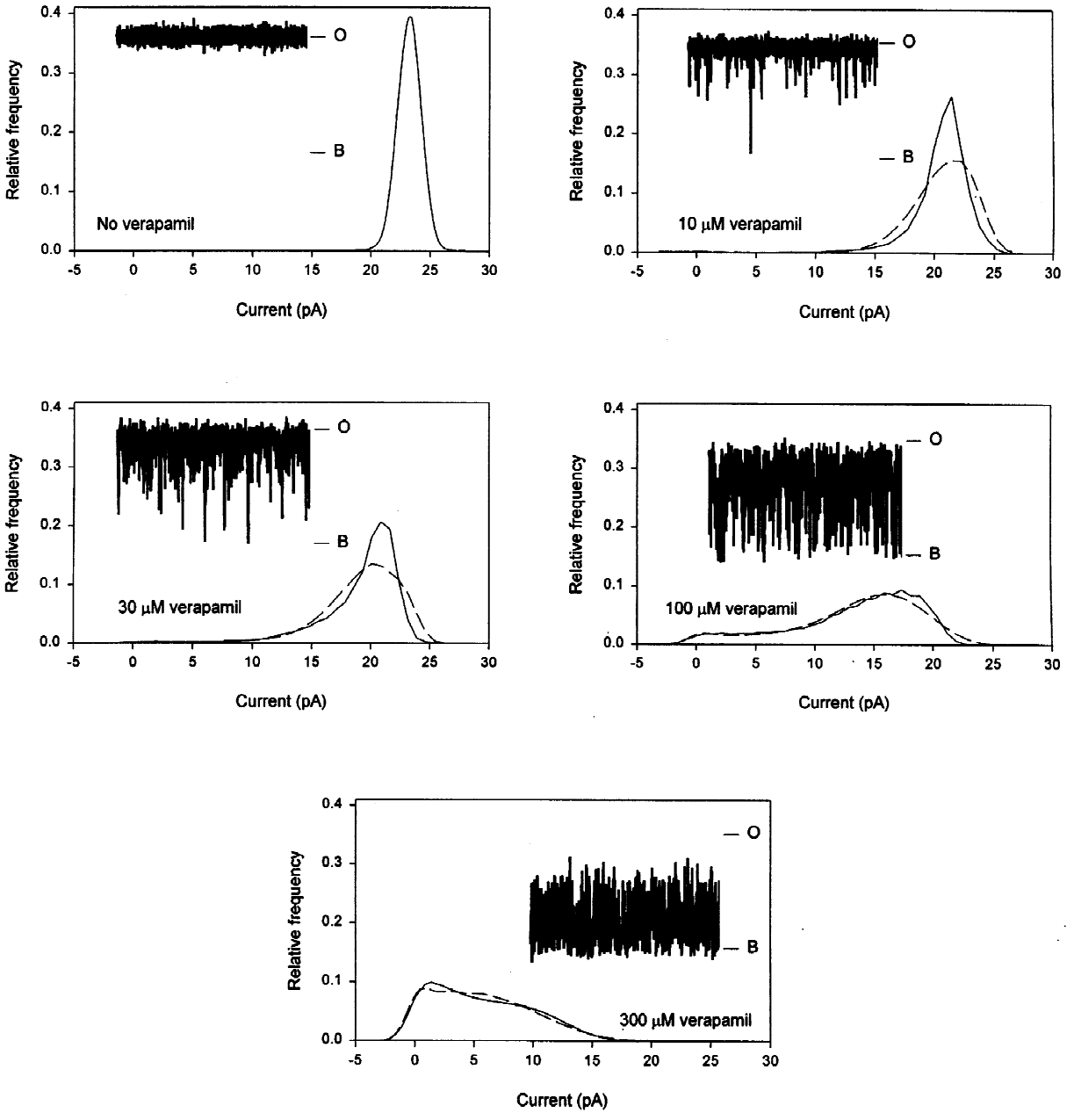

Fig. 5. The effect on current frequency distributions of increasing the verapamil concentration on the *trans* (cytoplasmic) side of the maxi cation channel. Currents were recorded at 70 mV in the presence of symmetrical 100 mM KCl. The observed current frequency distribution (—) is compared with that determined for a three-state $B1 \rightleftharpoons O \rightleftharpoons B2$ model (– – –) calculated with the values of unitary current presented in Fig. 3, a standard deviation of the current noise which averaged 1.01 pA and the rate constants presented in Fig. 7. *Inset:* Sample of the original current recordings (300 μsec in duration) filtered using an 8-pole Bessel filter set at 4 kHz. The current associated with channel open (*O*) and blocked (*B*) states is indicated.

be prerecorded and stored on DAT or videotape. Second, it does not rely on any correction for missed events. Finally, it is economical with computer time compared with methods involving the direct modelling of current records.

It would be interesting to compare rate constants obtained for the simple two-state model from the analysis of distributions of current-amplitude presented in this paper with those obtained by the technique described by Yellen (1984). It would also be instructive to compare results for multistate models obtained by the method presented here with those obtained using methods based on

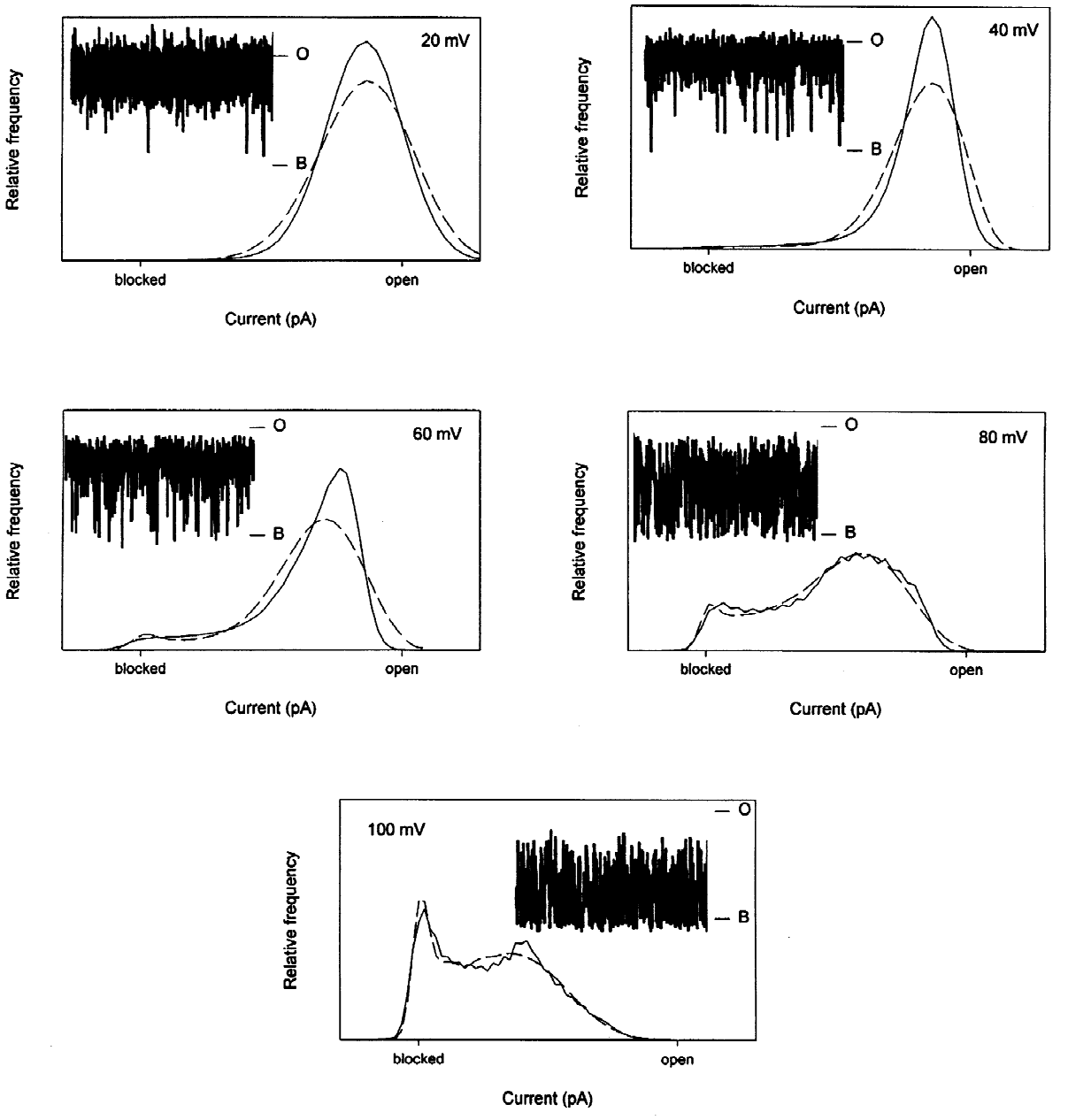

Fig. 6. The effect on current frequency distributions of increasing voltage at a verapamil concentration on the *trans* (cytoplasmic) side of the maxi cation channel of 100 μ*M*. Currents were recorded in the presence of symmetrical 100 mM KCl. The observed current frequency distribution (——) is compared with that determined for a three-state $B1 \rightleftharpoons O \rightleftharpoons B2$ model (– – –) calculated with the values of unitary current presented in Fig. 3, a standard deviation of the current noise which averaged 1.01 pA and the rate constants presented in Fig. 7. *Inset:* Sample of the original current recordings (300 μsec in duration) filtered using an 8-pole Bessel filter set at 4 kHz. The current associated with channel open (*O*) and blocked (*B*) states is indicated.

the presence of a single first-order filter (Rießner & Hansen, 1995) or by modelling the time series directly (Fredkin & Rice, 1992*a*). Such comparisons will be the subject of future work.

This work was supported by the Biotechnology and Biological Sciences Research Council (UK). We thank Prof. John Rice (University of California, CA, USA), Dr. Tony Fisher (University of York, UK) and Prof. Howell Tong (University of Kent, UK) for helpful discussions about filtering, and Prof. R.S. Eisenberg and Dr. R. Levis (Rush University, Chicago, IL, USA) for help in simulating electrical noise. We also thank Prof. M.A. Venis and Mr. J.S. Fenlon (both HRI) for their comments on early versions of this manuscript.

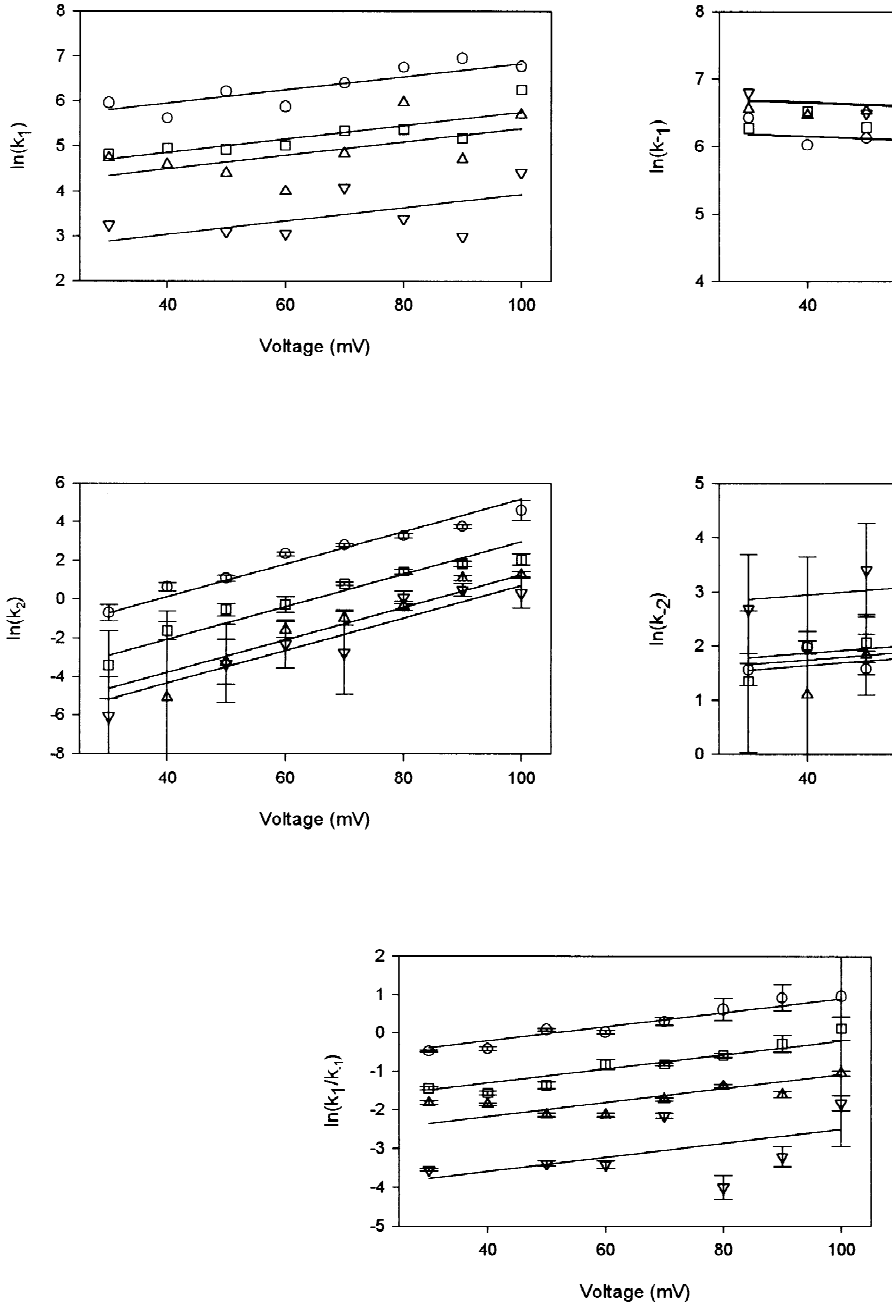

Fig. 7. The relationship between the rate constants for the *B1* ⇌ *O* ⇌ *B2* kinetic model and voltage. The rate constants ($msec^{-1}$) for blockade of the open channel by verapamil are indicated by k_1 and k_2, and the rates at which the channel is unblocked by k_{-1} and k_{-2}, the subscripts referring to the two independent blocked states *B1* and *B2* respectively. Data were obtained at verapamil concentrations in the *trans* (cytoplasmic) chamber of 10 μM (▽), 30 μM (△), 100 μM (□) and 300 μM (○). Standard errors for rate constants are indicated by vertical bars, but are not presented for k_1 and k_{-1} because they were erratic and frequently very large. However, the estimates had a high negative correlation and the standard error of $\ln(k_1/k_{-1})$ was generally small. The fitted lines are parallel regression curves. Intercepts for k_1 were 2.45 (10 μM), 3.90 (30 μM), 4.26 (100 μM) and 5.35 (300 μM), and the slope was 0.0148. Intercepts for k_{-1} were 6.78 (10 μM), 6.79 (30 μM), 6.29 (100 μM) and 6.28 (300 μM), and the slope was −0.0034. Intercepts for k_2 were −7.70 (10 μM), −7.16 (30 μM), −5.44 (100 μM) and −3.24 (300 μM), and the slope was 0.084. Intercepts for k_{-2} were 2.61 (10 μM), 1.40 (30 μM), 1.30 (100 μM) and 1.53 (300 μM), and the slope was 0.0085. For $\ln(k_1/k_2)$ intercepts were −4.32 (10 μM), −2.89 (30 μM), −2.03 (100 μM) and −0.93 (300 μM), and the slope was 0.0182.

References

Albertsen, A., Hansen, U.-P. 1994. Estimation of kinetic rate constants from multi-channel recordings by a direct fit of the time series. *Biophys. J.* **67:**1393–1403

Ball, F.G., Davies, S.S. 1995. Statistical inference for a two-state Markov model of a single ion channel, incorporating time interval omission. *J. Roy. Statistical Soc. B* **57:**269–287

Bertl, A., Blumwald, E., Coronado, R., Eisenberg, R., Findlay, G., Gradmann, D., Hille, B., Köhler, K., Kolb, H.-A., MacRobbie, E., Meissner, G., Miller, C., Neher, E., Palade, P., Pantoja, O., Sanders, D., Schroeder, J., Slayman, C., Spanswick, R., Walker, A., Williams, A. 1992. Electrical measurements on endomembranes. *Science* **258:**873–874

Catterall, W.A., Striessnig, J. 1992. Receptor sites for Ca^{2+} channel antagonists. *TIPS* **13:**256–262

Chung, S.H., Moore, J.B., Xia, L., Premkumar, L.S., Gage, P.W. 1990. Characterization of single channel currents using digital signal-processing techniques based on Hidden Markov Models. *Phil. Trans. Roy. Soc. London B* **329:**265–285

Colquhoun, D. 1994. Practical analysis of single channel records. *In:* Microelectrode Techniques. The Plymouth Workshop Handbook. D. Ogden, editor. pp. 101–139. Company of Biologists, Cambridge

Colquhoun, D., Hawkes, A.G. 1981. On the stochastic properties of single ion channels. *Proc. Roy. Soc. London B* **211:**205–235

Colquhoun, D., Sigworth, F.J. 1983. Fitting and statistical analysis of single-channel records. *In:* Single-Channel Recording. B. Sakmann and E. Neher, editors. pp. 191–264. Plenum, New York

Cox, D.R., Miller, H.D. 1965. The Theory of Stochastic Processes. Chapman & Hall, London

Draber, S., Hansen, U.-P. 1994. Fast single-channel measurements resolve the blocking effect of Cs^+ on the K^+ channel. *Biophys. J.* **67:**120–129

Draber, S., Schultze, R. 1994. Correction for missed events based on a realistic model of a detector. *Biophys. J.* **66:**191–201

Ertel, E.A., Cohen, C.J. 1994. Voltage-dependent interactions: The influence and significance of membrane potential on drug-receptor interactions. *Drug Devel. Res.* **33:**203–213

FitzHugh, R. 1983. Statistical properties of the asymmetric random telegraph signal, with applications to single-channel analysis. *Math. Biosci.* **64:**75–89

Fredkin, D.R., Rice, J.A. 1992*a*. Maximum likelihood estimation and identification directly from single-channel recordings. *Proc. Roy. Soc. London B* **249:**125–132

Fredkin, D.R., Rice, J.A. 1992*b*. Bayesian restoration of single-channel patch clamp recordings. *Biometrics* **48:**427–448

Heinemann, S.H., Sigworth, F.J. 1988. Open channel noise. IV. Estimation of rapid kinetics of formamide block in gramicidin A channels. *Biophys. J.* **54:**757–764

Heinemann, S.H., Sigworth, F.J. 1991. Open channel noise. VI. Analysis of amplitude histograms to determine rapid kinetic parameters. *Biophys. J.* **60:**577–587

Hille, B. 1992. Ionic Channels of Excitable Membranes. Sinauer Associates, Sunderland, MA

Horn, R., Lange, K. 1983. Estimating kinetic constants from single channel data. *Biophys. J.* **43:**207–223

Kienker, P. 1989. Equivalence of aggregated Markov models of ion-channel gating. *Proc. Roy. Soc. London B* **236:**269–309

Klieber, H.-G., Gradmann, D. 1993. Enzyme kinetics of the prime K^+ channel in the tonoplast of *Chara:* selectivity and inhibition. *J Membrane Biol.* **132:**253–265

McCullagh, P., Nelder, J.A. 1989. Generalized Linear Models. Chapman and Hall, London

Miller, C. 1982. Open-state substructure of single chloride channels from *Torpedo* electroplax. *Phil. Trans. Roy. Soc. London B* **299:** 401–411

Moler, C., Van Loan, C. 1978. Nineteen dubious ways to compute the exponential of a matrix. *SIAM Review* **20:**801–836

Nelder, J.A., Mead, R. 1965. A simplex method for function minimization. *Computer J.* **7:**308–313

Pietrobon, D., Prod'hom, B., Hess, P. 1989. Interactions of protons with single open L-type calcium channels. pH-dependence of proton-induced current fluctuations with Cs^+, K^+ and Na^+ as permeant ions. *J. Gen. Physiol.* **94:**1–21

Piñeros, M., Tester, M. 1995. Characterization of a voltage-dependent Ca^{2+}-selective channel from wheat roots. *Planta* **195:**478–488

Rabiner, L.R. 1989. A tutorial on hidden Markov models and selected applications in speech recognition. *Proc. Inst. Elect. Eng.* **77:**257–285

Rießner, T., Hansen, U.-P. 1995. Fast switching in patch clamp records as analyzed by an extended theory of multi-state multi-channel beta distributions. *In:* Abstracts of the 10th International Workshop on Plant Membrane Biology, Regensburg

Roberts, A.W., Haigler, C.H. 1990. Tracheary-element differentiation in suspension-cultured cells of *Zinnia* requires uptake of extracellular Ca^{2+}. Experiments with calcium-channel blockers and calmodulin inhibitors. *Planta* **180:**502–509

Schultze, R., Draber, S. 1993. A nonlinear filter algorithm for the detection of jumps in patch-clamp data. *J. Membrane Biol.* **132:**41–52

Thomine, S., Zimmermann, S., Van Duijn, B., Barbier-Brygoo, H., Guern, J. 1994. Calcium channel antagonists induce direct inhibition of the outward rectifying potassium channel in tobacco protoplasts. *FEBS Lett.* **340:**45–50

White, P.J. 1993. Characterization of a high-conductance, voltage-dependent cation channel from the plasma membrane of rye roots in planar lipid bilayers. *Planta* **191:**541–551

White, P.J. 1996. Specificity of ion channel inhibitors for the maxi cation channel in rye root plasma membranes. *J. Exp. Bot.* **47:**713–716

White, P.J., Smahel, M., Thiel, G. 1993. Characterization of ion channels from *Acetabularia* plasma membrane in planar lipid bilayers. *J Membrane Biol.* **133:**145–160

White, P.J., Tester, M.A. 1992. Potassium channels from the plasma membrane of rye roots characterized following incorporation into planar lipid bilayers. *Planta* **186:**188–202

White, P.J., Tester, M. 1994. Using planar lipid-bilayers to study plant ion channels. *Physiol. Plant.* **91:**770–774

Woodhull, A.M. 1973. Ionic blockage of sodium channels in nerve. *J. Gen. Physiol.* **61:**687–708

Yellen, G. 1984. Ionic permeation and blockade in Ca^{2+}-activated K^+ channels of bovine chromaffin cells. *J. Gen. Physiol.* **84:**157–186